



Pergamon

Acta Materialia 50 (2002) 2933–2944



www.actamat-journals.com

Relaxation of compressed elastic islands on a viscous layer

J. Liang^a, R. Huang^a, H. Yin^b, J.C. Sturm^b, K.D. Hobart^c, Z. Suo^{a,*}

^a Department of Mechanical Engineering and Princeton Materials Institute, Princeton University, Princeton, NJ 08544, USA

^b Center for Photonics and Optoelectronic Materials and Department of Electrical Engineering, Princeton University, Princeton, NJ 08544, USA

^c Naval Research Laboratory, Washington, DC 20375, USA

Received 8 November 2001; accepted 5 February 2002

Abstract

A recent technique can fabricate SiGe thin film islands on a glass layer, which itself lies on a silicon wafer. The islands initially have an inplane compressive strain. Upon annealing, the glass flows, and the islands relax. The resulting strain-free islands are used as substrates to grow epitaxial optoelectronic devices. This paper models the annealing process. A small island relaxes by inplane expansion. The glass being viscous, the relaxation starts at the island edges, and propagates to the island center. A large island, however, wrinkles at the center before the inplane relaxation arrives. Further annealing gives rise to one of two outcomes. The wrinkles may disappear when the inplane relaxation arrives, leading to a flat, strain-free island. Alternatively, the wrinkles may cause significant tensile stress in the island, leading to fracture. We model the island by the von Karman plate theory, and the glass layer by the Reynolds lubrication theory. The solid and the fluid couple at the interface by the continuous traction and displacement. Numerical simulations evolve the inplane expansion and the wrinkles simultaneously. We determine the critical island size, below which inplane expansion prevails over wrinkling. This critical island size depends on several experimental variables, and is much larger than the Euler buckling wavelength. © 2002 Acta Materialia Inc. Published by Elsevier Science Ltd. All rights reserved.

Keywords: Compliant substrate; Thin films; Strain relaxation; Wrinkling; Viscous flow

1. Introduction

For nearly half a century, Si has been the prevailing substrate in the microelectronic industry. Integrating other materials on Si has been a persistent challenge. Recently, various “compliant substrates” have been fabricated for optoelectronic applications [1]. Fig. 1 illustrates one fabrication

process [2,3]. First grow an epitaxial SiGe film on an Si host wafer. Because SiGe has a larger lattice constant than Si, the SiGe film is compressively strained, and is made very thin to avert threading dislocations [4]. Separately prepare a layer of borophosphosilicate glass (BPSG) on an Si handle wafer. Stack the two wafers by the wafer bonding method, with SiGe facing the BPSG. Subsequently remove the Si host wafer, and pattern the SiGe film into islands. At this stage, the SiGe islands remain strained because the island size is much larger than the island thickness, and the BPSG is solid at room temperature. Upon annealing above the glass tran-

* Corresponding author. Tel.: +1-609-258-0250; fax: +1-609-258-5877.

E-mail address: suo@princeton.edu (Z. Suo).

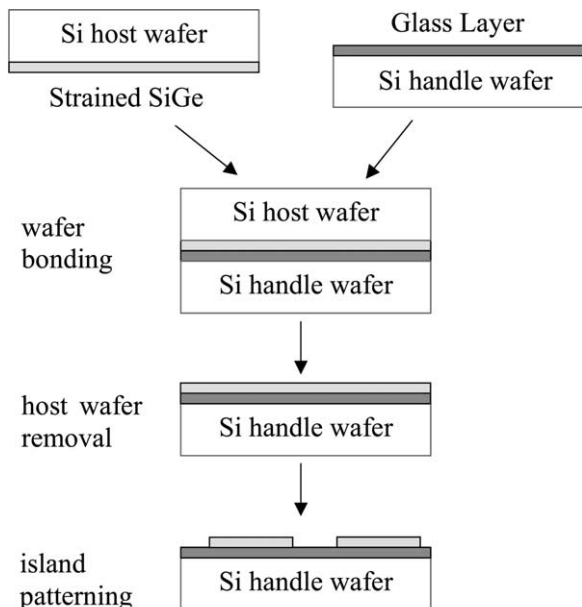


Fig. 1. Schematic of the SiGe island fabrication process.

sition temperature of BPSG, the glass layer flows, and the islands relax. The goal is to obtain flat, strain-free islands, on which one can grow epitaxial optoelectronic devices with SiGe or other semiconductors of a similar lattice constant. Because the islands and the devices on them are strain-free, they can be of any thickness without acquiring threading dislocations. Large islands are desired; the larger each island is, the more devices it can accommodate.

This paper models the annealing process. Fig. 2 illustrates the salient experimental observations [2,3]. Before annealing, an island is flat and under an inplane compressive strain (Fig. 2a). At the annealing temperature, the island deforms elastically, dragging the glass layer underneath to creep by viscous flow. The island remains bonded to the glass. If the island is small, it expands in its plane and remains flat (Fig. 2b). If the island is large, it wrinkles (Fig. 2c). In the drawing, the lateral length has been greatly contracted compared to the vertical length. Upon further annealing, the wrinkles may disappear when inplane relaxation reaches the island center. Alternatively, the wrinkles may become so severe that high tensile stress arises in the island, leading to fracture.

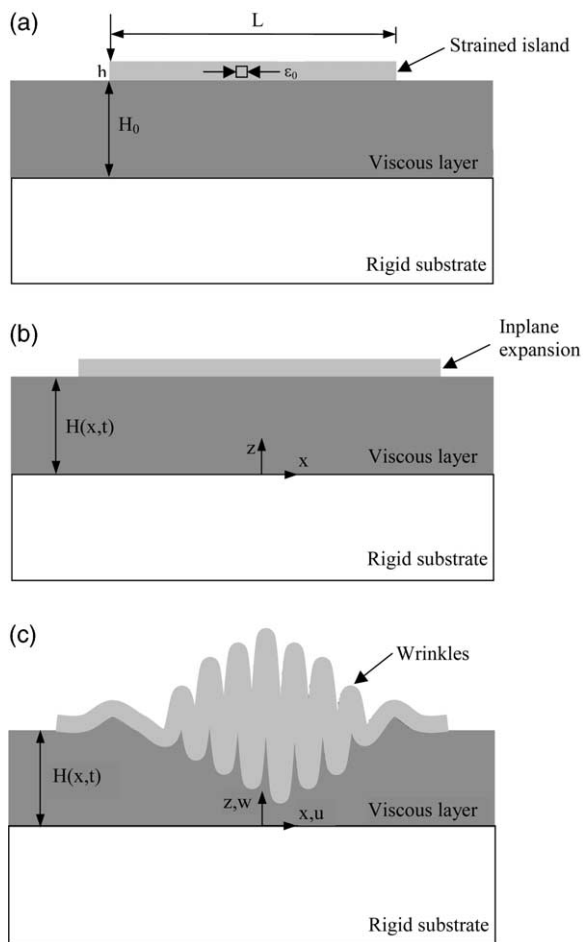


Fig. 2. Annealing behaviors of the island. (a) The flat island is initially biaxially strained. (b) Effect of just inplane expansion. (c) Effect of wrinkling at the center and expansion at the edges. In the drawings, the horizontal length is greatly contracted compared to the vertical length.

Everything else being equal, a critical island size exists, below which the island relaxes without wrinkle-fracture.

These experimental observations have inspired several theoretical studies. Freund and Nix [5] formulated a shear lag model, which accounted for inplane expansion but neglected wrinkling. Sridhar et al. [6] studied wrinkling but excluded inplane expansion. Huang and Suo [7,8] and Sridhar et al. [9] examined both inplane and out-of-plane displacements during wrinkling. However, they

assumed that the SiGe film was infinite, precluding net inplane expansion.

Building on previous experimental and theoretical work, this paper aims to identify the critical island size. We model the viscous layer by the Reynolds lubrication theory, and the elastic island by the von Karman nonlinear plate theory. Section 2 describes the partial differential equations, the boundary conditions at the island edges, and the numerical method. Section 3 describes simulations of islands of different sizes. To place the numerical results in context, we review the relevant theoretical results. Section 4 compares the time scales of inplane expansion and of wrinkling, and predicts the critical island size as a function of experimental variables. Section 5 shows stresses developed in the island and the viscous layer. This paper focuses on the model, using experimental observations to motivate several considerations. We leave quantitative comparison between the model and the experiment to a separate paper.

2. The model

The island relaxes in both the x and y directions. However, to simplify the model, this paper will consider only the relaxation in the x direction, under the plane strain conditions. The film has membrane displacement $u(x,t)$ and deflection displacement $w(x,t)$ (Fig. 2c). Let H_0 be the thickness of the glass layer when it is flat. Once the island wrinkles, dragging the glass underneath, the thickness of the glass layer becomes nonuniform, $H(x,t) = H_0 + w(x,t)$. The elastic island and the viscous layer interact through the pressure $p(x,t)$ and the shear stress $T(x,t)$ on the interface.

The glass layer is modeled as an incompressible Newtonian fluid with viscosity η , creeping slowly between two nearly parallel surfaces. The thickness of the glass layer is small compared to the characteristic horizontal length scale, such as the wrinkling wavelength. Consequently, the Reynolds lubrication theory [10] adequately describes the BPSG layer. This theory reduces the three spatial coordinates in the Navier–Stokes equations to only one spatial coordinate x . The lubrication theory has been adapted to various situations over the last cen-

tury. Within the present context, the governing equations are [7]

$$\frac{\partial w}{\partial t} = \frac{\partial}{\partial x} \left(\frac{H^3 \partial p}{3\eta \partial x} - \frac{H^2}{2\eta} T \right), \tag{1}$$

$$\frac{\partial u}{\partial t} = -\frac{H^2 \partial p}{2\eta \partial x} + \frac{H}{\eta} T. \tag{2}$$

Eqs. (1) and (2) relate the velocities, $\partial w/\partial t$ and $\partial u/\partial t$, to the tractions, p and T .

To evolve these equations, we need to express the tractions p and T in terms of the displacements u and w . We model the island by the von Karman nonlinear plate theory [11: pp. 57–60, 12: pp. 378–380]. We take the flat island under biaxial inplane strain ϵ_0 to be the reference state, in which $u = w = 0$. The membrane force in the island relates to the displacements as

$$N = \frac{E\epsilon_0 h}{(1-\nu)} + \frac{Eh}{1-\nu^2} \left[\frac{\partial u}{\partial x} + \frac{1}{2} \left(\frac{\partial w}{\partial x} \right)^2 \right], \tag{3}$$

where h is the island thickness, E is Young’s Modulus, and ν is Poisson’s ratio. Under the plane–strain conditions, force and moment balance demand that

$$T = \frac{\partial N}{\partial x}, \tag{4}$$

$$p = D \frac{\partial^4 w}{\partial x^4} - N \frac{\partial^2 w}{\partial x^2} - T \frac{\partial w}{\partial x}, \tag{5}$$

where D is the flexural rigidity of the elastic island,

$$D = \frac{Eh^3}{12(1-\nu^2)}.$$

The length of the island is L . The free edges of the island allow the island to expand in its plane. The boundary conditions at the two island edges, $x = \pm L/2$, are:

No membrane force,

$$\frac{E\epsilon_0 h}{(1-\nu)} + \frac{Eh}{1-\nu^2} \left[\frac{\partial u}{\partial x} + \frac{1}{2} \left(\frac{\partial w}{\partial x} \right)^2 \right] = 0. \tag{6}$$

No moment, $\frac{\partial^2 w}{\partial x^2} = 0$.

No shear force, $\frac{\partial^3 w}{\partial x^3} = 0$. (8)

$$\text{No pressure, } D \frac{\partial^4 w}{\partial x^4} - T \frac{\partial w}{\partial x} = 0. \quad (9)$$

Eqs. (1)–(5) complete the governing equations for a strained elastic island on a viscous layer. At a given time, assume u and w are known. Eqs. (3)–(5) give p and T at the time, and eqs. (1) and (2) update u and w for a small time step. The procedure is repeated for many time steps to evolve the system over a long time.

When the island is fully relaxed, the displacements become

$$w = \text{constant}, u = -(1 + \nu)\varepsilon_0 x, \quad (10)$$

and $p = N = T = 0$. This state satisfies all the governing equations and the boundary conditions. During relaxation, because shear stress is nonuniform, a net amount of glass under the island center flows to the edges. Consequently, the island will sink somewhat during relaxation.

In the numerical simulations, we use $H_0 = 200\text{nm}$, $h = 30\text{nm}$, $\nu = 0.3$, $\varepsilon_0 = -0.012$, corresponding to one set of experimental conditions in [2,3]. Time is normalized by η/E . We set the initial conditions to be

$$u(x,0) = 0, w(x,0) = A_0 \cos(kx), \quad (11)$$

where A_0 is the initial amplitude, and k is the wavenumber. We set $A_0/h = 0.001$ and $kh = 0.314$. This particular wavenumber is close to the wavenumber at which the perturbation amplifies most rapidly. The qualitative outcome is insensitive to the initial amplitude. These matters will be further discussed later.

We use an implicit finite difference scheme. At each edge, to satisfy the boundary conditions, three fictitious nodes are added, one for u and the other two for w . The resulting system of nonlinear algebraic equations is solved using the Newton method. Convergence tests show that $\Delta x/h = 0.125$ and $\Delta t = 0.1\eta/E$ are suitable.

3. Relaxation of islands of different sizes

This section presents the results of numerical simulation and discusses them in light of available theoretical models and experimental observations.

Islands of three sizes, $L = 15, 30, 60 \mu\text{m}$, are simulated. We label them as small, intermediate, and large islands. The significance will become clear shortly.

3.1. A small island

Fig. 3 shows the numerical results for a small island, $L = 15\mu\text{m}$. The membrane displacement u at the edges quickly increases and then gradually reaches the fully relaxed magnitude. In the plots for deflection, w is normalized by h , and x by $L/2$. Because $L \gg h$, the horizontal length appears greatly contracted compared to the vertical length. The deflection exhibits some roughness, with amplitudes much less than h . Clearly, when the island is small, inplane expansion rapidly travels from the edges to the center of the island, so that wrinkles have little time to grow. To conserve mass, the edges bend downward initially, and then the entire island sinks by $0.05 h$. The initial edge bending-down has been observed experimentally [2,3], but overall island sinking has not been reported.

Remarkably, the inplane expansion suppresses the wrinkles even when the island size is many times the critical wavelength of the Euler buckling. The latter is given by [6]

$$k_c h = \sqrt{-12\varepsilon_0(1 + \nu)}. \quad (12)$$

For this simulation, $k_c h = 0.433$, which is above the wavenumber of the initial perturbation $kh = 0.314$. Consequently, the amplitude of the deflection grows before inplane relaxation reaches the island center (Fig. 3). Even though the critical wavelength, $\lambda_c = 2\pi/k_c = 0.436\mu\text{m}$, is considerably smaller than the island size, $L = 15\mu\text{m}$, the inplane relaxation reaches the center fast enough to prevent significant wrinkling. In experiments [1,2], wrinkles were not appreciable for islands with $L < 30\mu\text{m}$.

The island is said to have relaxed when the membrane force at the center has dropped by more than 99.9% of its initial value. The simulations indicate that the time for the $15 \mu\text{m}$ film to reach the relaxed state is $24901.5 \eta/E$. Take $\eta = 15\text{GPa}\cdot\text{s}$ and $E = 200\text{GPa}$, the island is completely relaxed in about 30 min.

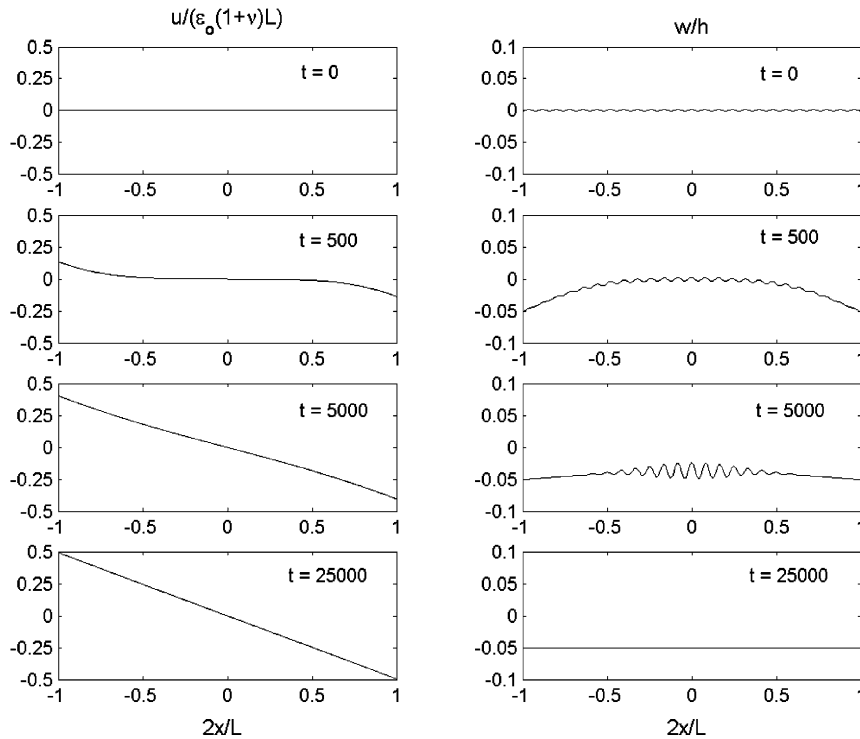


Fig. 3. Simulation results for a 15 μm film. The membrane displacement and deflection distributions at different times.

As observed in experiments [2,3] and in the above numerical simulation, small islands relax by inplane expansion and remain nearly flat. Consequently, for small islands, we can neglect deflection w in eqs. (1)–(5). At time zero, the island has biaxial strain ϵ_0 , the membrane force $N = E\epsilon_0 h / (1 - \nu)$, and the displacement $u = 0$. When the island is completely relaxed, the membrane force is $N = 0$, and the membrane displacement is $u = -(1 + \nu)\epsilon_0 x$. The shear lag model [5] reproduced below describes the transient process from the initial state to the relaxed state.

Fig. 4 illustrates the shear lag model. Force balance of a differential element of the island requires that

$$T = \frac{\partial N}{\partial x}. \tag{13}$$

The island is elastic, so that the membrane force N relates to the mismatch strain and the displacement gradient by Hooke’s law:

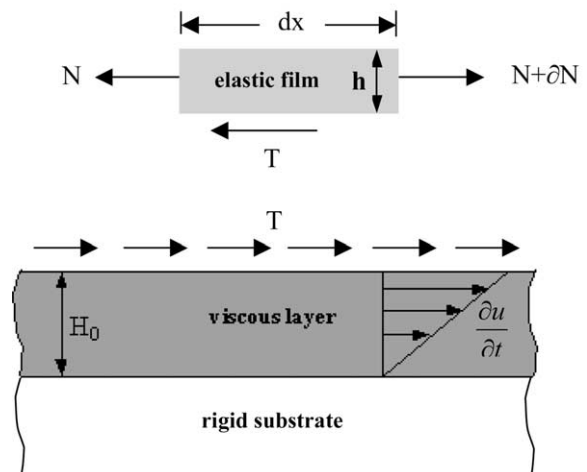


Fig. 4. The shear lag model. Force balance on an element of the elastic island, and viscous shear flow in the glass layer.

$$N = \frac{E\varepsilon_0 h}{(1-\nu)} + \frac{Eh}{(1-\nu^2)} \frac{\partial u}{\partial x}. \quad (14)$$

The viscous layer has a linear velocity profile, so that the shear stress relates to the velocity as

$$T = \frac{\eta}{H_0} \frac{\partial u}{\partial t}. \quad (15)$$

Eqs. (13)–(15) can also be obtained from eqs. (2)–(4) by setting $p = 0$ and $w = 0$. That is, the shear lag model is a special case of the more general model described in Section 2.

Combining eqs. (13)–(15), one finds that

$$\frac{\partial u}{\partial t} = \Omega \frac{\partial^2 u}{\partial x^2}, \quad (16)$$

where

$$\Omega = \frac{EH_0 h}{(1-\nu^2)\eta}.$$

Eq. (16) is identical to the diffusion equation once Ω is identified as the diffusivity. The boundary conditions are

$$N = 0 \text{ at } x = \pm L/2, \quad (17)$$

Subject to the initial and the boundary conditions, the displacement field evolves as [5]

$$u(x,t) = -\varepsilon_0(1+\nu) \left[x - \sum_{n=0}^{\infty} A_n \sin(k_n x) \exp(-\Omega k_n^2 t) \right], \quad (18)$$

where

$$k_n = \frac{(2n+1)\pi}{L}, \quad (19)$$

$$A_n = (-1)^n \frac{L}{\pi^2(n+1/2)^2}. \quad (20)$$

When $t \rightarrow \infty$, eq. (18) recovers the relaxed state $u = -(1+\nu)\varepsilon_0 x$. Also plotted in Fig. 3 is the membrane displacement computed from the shear lag model, eq. (18), which is indistinguishable from the numerical results.

3.2. An intermediate island

Fig. 5 plots the displacements for an intermediate island, $L = 30\mu\text{m}$. The shear lag prediction of the membrane displacement still agrees reasonably with that obtained from the numerical simulations. Note that, for the w plots, the scales in Figs. 3 and 5 are different. Now the island is large enough so that wrinkles are manifest on the order h , but persist only for a period of time.

Fig. 6 shows the membrane force and shear stress distributions for the same island, $L = 30\mu\text{m}$. The stresses are normalized by the compressive stress before relaxation. The membrane force decreases with time, is highest at the center, and approaches zero once fully relaxed. The membrane force vanishes at the two edges at all time due to the boundary conditions. Observe that before inplane expansion from the island edges reaches the island center, the membrane force has already been partially relaxed by wrinkling. The numerical result is quite different from that of the shear lag model. The shear stress distribution is anti-symmetric about the island center. At each point, the glass flows in the same direction as the shear stress. The gradient of the shear stress signifies the vertical velocity at a particular point.

The island at $t = 160000\eta/E$ has a depression at the center, comparable to one long and flat wave (Fig. 5). The amplitude of this wave is about 20 nm, but occurs over a distance of about $15\mu\text{m}$. The time to reach the relaxed state (i.e., below 0.1% the initial membrane force) is about $105604.5\eta/E$ or 132 min.

3.3. A large island

A large island ($L = 60\mu\text{m}$) simulation is shown in Fig. 7. The membrane displacement u has minute undulations at the island center. A large part of the island now wrinkles. The shear lag model still reasonably describes the evolution trend of the membrane displacement, although the wrinkled island does fall behind in its inplane expansion compared with that predicted by the shear lag model. In what follows, we will mainly consider the characteristics of the wrinkling process.

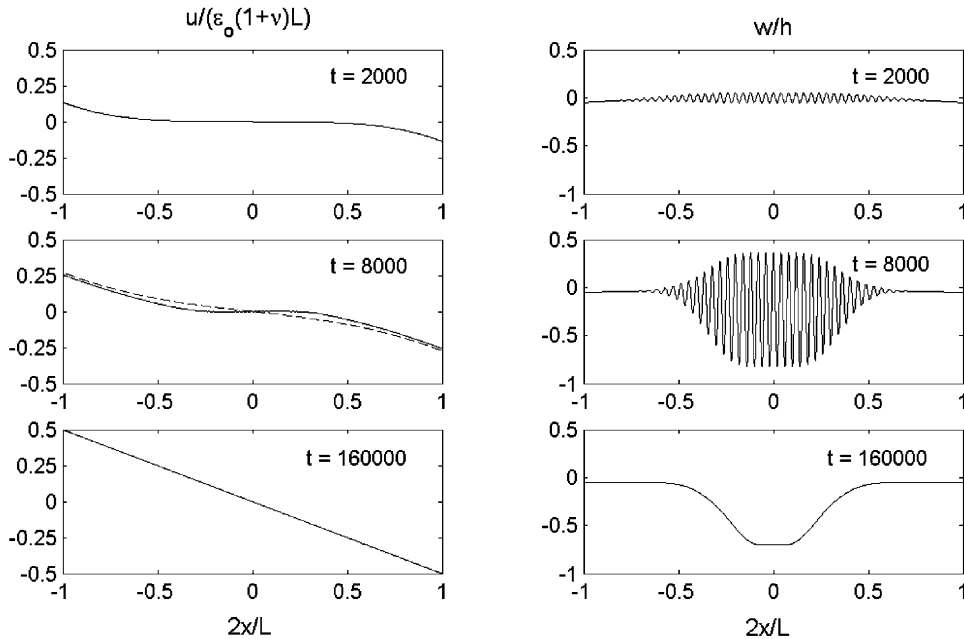


Fig. 5. Simulation results for a 30 μm film. The membrane displacement and deflection distributions at different times. Dashed lines in the displacement plots are from the shear lag model.

Huang and Suo [7] have carried out a linear perturbation analysis for an infinite film. Starting with a flat biaxially strained state, $u = w = 0$, $N = E\epsilon_0 h / (1 - \nu)$, and $p = T = 0$, both velocities $\partial u / \partial t$ and $\partial w / \partial t$ are zero. The film does not evolve. However, this equilibrium state is unstable. Given a small perturbation at time zero, $w = A_0 \sin(kx)$, the film will evolve to reduce the strain energy. The linear perturbation analysis predicts that amplitude grows exponentially with time, $A(t) = A_0 \exp(st)$. The parameter s measures the growth rate. When the wavenumber k is small, matter has to flow over a long distance to affect wrinkling, so that s is small. When the wavenumber k exceeds the Euler critical wavenumber k_c , the bending raises too much elastic energy and the deflection amplitude decays, so that s becomes negative. Consequently, s reaches a positive, maximum value s_m at an intermediate wavenumber k_m . Among perturbations of all wavenumbers, the perturbation of wavenumber k_m will grow most rapidly. The linear perturbation analysis gives $k_m h = 0.353$ for the numerical values used in this paper. In our numerical simul-

ation, we have used wavenumber $kh = 0.314$, which is close to $k_m h$.

For an infinite film, if the wavenumber of the perturbation is below the Euler critical wavenumber, $k < k_c$, the film will evolve to a kinetically constrained equilibrium state [6,7]. The viscous layer stops flowing and the tractions vanish (i.e., $p = T = 0$); the film remains in a wrinkled state. The amplitude at the constrained equilibrium state takes the form

$$A_{eq} = h \sqrt{\frac{1}{3} \left[\left(\frac{k_c}{k} \right)^2 - 1 \right]} \tag{21}$$

For this work, $A_{eq} = 12.3\text{nm}$. Wrinkles observed in the experiments may correspond to one of these constrained equilibrium states.

Fig. 8 plots the numerical results of the normalized amplitude at the island center versus the normalized time. Also plotted are the predictions according to the constrained equilibrium state (CE), and according to the linear perturbation analysis (LP). For the 15 μm island, the simulation

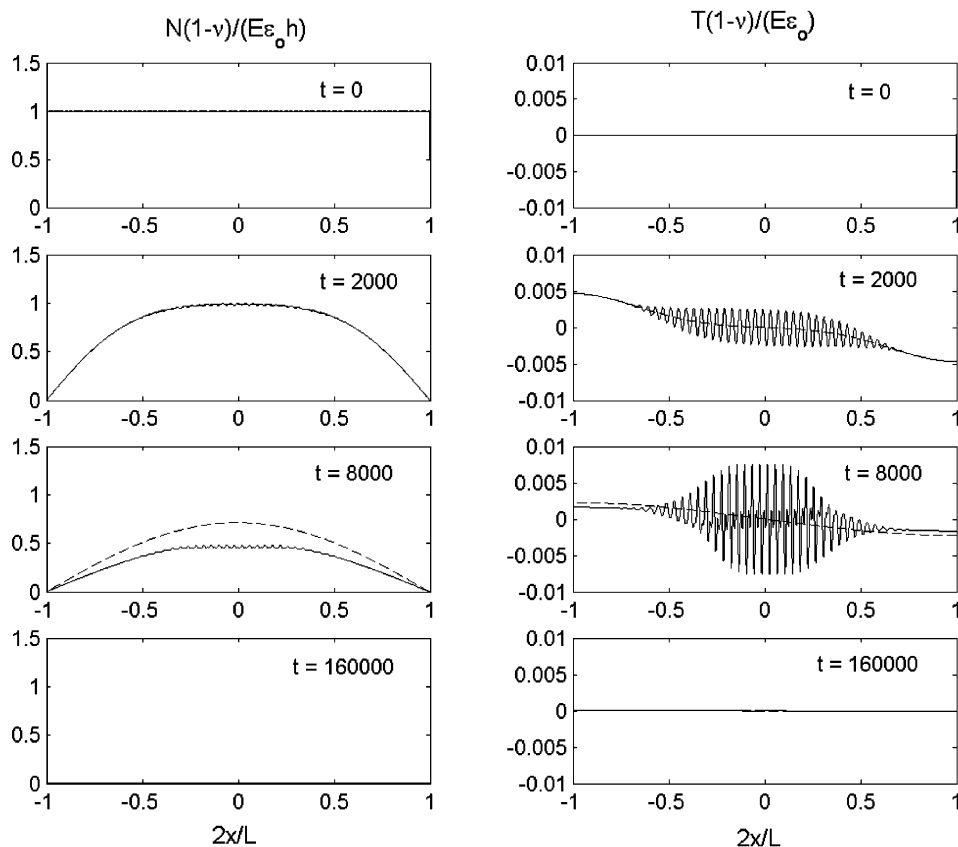


Fig. 6. Simulation results for a 30 μm film. The membrane force and shear stress distributions at different times. Dashed lines in the membrane force and shear stress plots are from the shear lag model.

matches well to LP in short times. The amplitude increases somewhat and then decreases when the inplane expansion reaches the island center. The wrinkles die out before reaching CE. For the 30 μm island, the simulation also matches well with LP initially, and attains CE after some time. However, after about 12000 η/E , the amplitude commences to decay. For the 60 μm island, CE persists for a much longer time. When the island is large enough for its center to attain CE, the time to get to the state is independent of the island size.

4. Critical island size

Both previous experiments [2,3] and the present simulations show that, everything else being equal, a critical island size L_c exists, below which the

island expands in its plane without significant wrinkling. Severe wrinkles cause tensile stress and fracture in the island and should be avoided during annealing. This section determines the critical island size as a function of experimental variables.

If inplane expansion prevails, the shear lag model gives a time scale:

$$t_E = \frac{L^2}{\pi^2 \Omega} = \frac{1-\nu^2}{\pi^2} \left(\frac{\eta}{E} \right) \left(\frac{L^2}{H_0 h} \right). \quad (22)$$

Here we use the relaxation time of the first term in the series in eq. (18). This expression has been obtained in [5]. As pointed out before, the relaxation time scales with η/E . A large island takes a long time to relax, as expected. A thin island decreases the stiffness of the system, and a thin glass layer reduces the flow rate for a given shear stress. Both effects prolong the relaxation time.

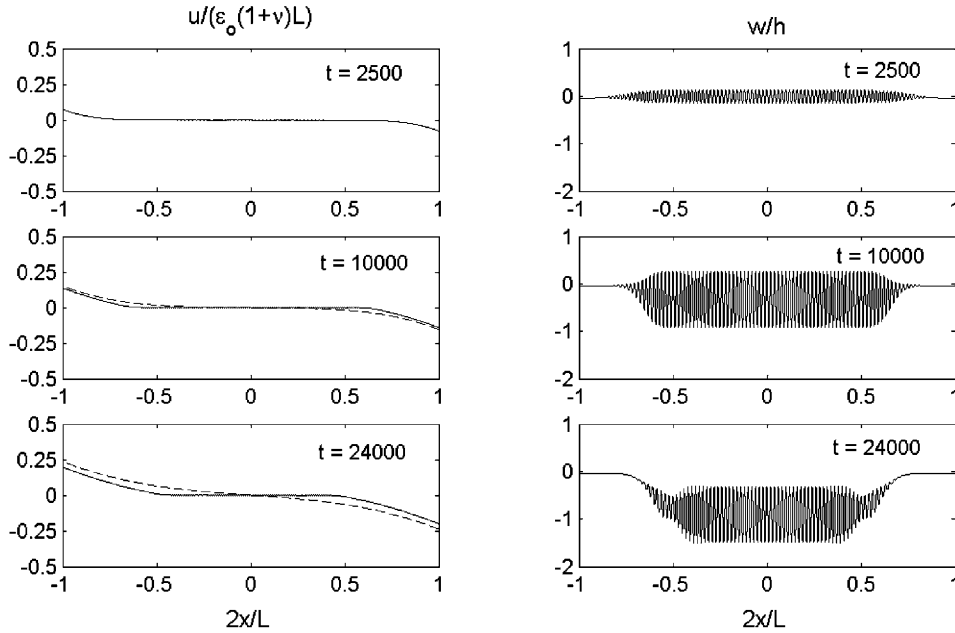


Fig. 7. Simulation results for a 60 μm film. The membrane displacement and deflection distributions at different times. Dashed lines in the displacement plots are from the shear lag model.

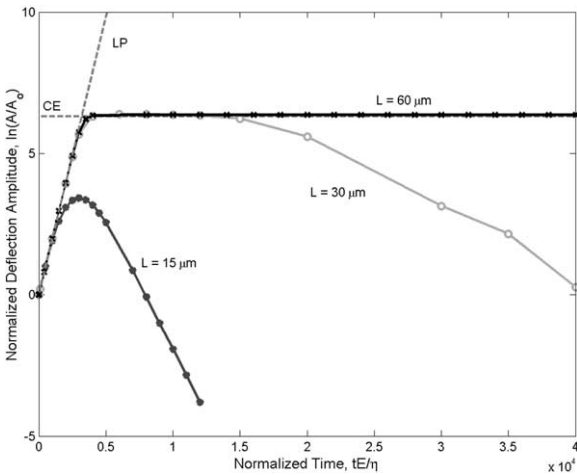


Fig. 8. Evolution of wrinkle amplitude. LP: linear perturbation. CE: constrained equilibrium.

Before the inplane expansion arrives, the island center wrinkles. As the numerical simulations show clearly, the wrinkling amplitude obeys the linear perturbation analysis, $A = A_0 \exp(st)$, up to the time the island is nearly at CE. To be conservative with over prediction of the critical island size,

we allow wrinkles to amplify in the fastest mode, so that $A = A_0 \exp(s_m t)$. Dimensional considerations demand that

$$s_m = \frac{f}{1-\nu^2} \left(\frac{E}{\eta} \right). \quad (23)$$

The dimensionless number f is a function of two variables, h/H and $\varepsilon_0(1 + \nu)$. The function is contained in Ref. [8], which models the glass layer exactly without using the lubrication approximation. For example,

$$f = \frac{1}{12} [-4\varepsilon_0(1 + \nu)]^{3/2}$$

when $h/H \rightarrow 0$, and

$$f = \frac{16}{9} \left[-\varepsilon_0(1 + \nu) \frac{H}{h} \right]^3$$

when $h/H \rightarrow \infty$. For the wrinkles to amplify from A_0 to A , the time needed is

$$t_w = \frac{1}{s_m} \ln \left(\frac{A}{A_0} \right) = \frac{(1-\nu^2)\eta}{f E} \ln \left(\frac{A}{A_0} \right). \quad (24)$$

The wrinkling time scale is also proportional to

η/E . As expected, before the inplane expansion arrives, the wrinkling time is independent of the island size L . To determine t_w , we need to know A_0 , and to declare what amplitude A constitutes a “severe” wrinkle. Fortunately, both A and A_0 appear in the logarithmic function, so that t_w is insensitive to the precise choice of A and A_0 .

We determine the critical island size, L_c , by setting $t_E = t_w$, so that

$$L_c = \pi \sqrt{\frac{H_0 h}{f} \ln\left(\frac{A}{A_0}\right)} \tag{25}$$

Because both t_E and t_w scale with η/E , the critical island size is independent of η/E . If one raises the annealing temperature and therefore decreases the viscosity, both the inplane expansion and wrinkling accelerate, but L_c remains unchanged. A large island will wrinkle and fracture whether it lies on a low viscosity polymer or on a high viscosity glass. Analytical results are available at two limits:

$$L_c = \pi \sqrt{12H_0 h \ln\left(\frac{A}{A_0}\right)} \tag{26}$$

$$[-4\varepsilon_0(1 + \nu)]^{-3/4}, \frac{h}{H} \rightarrow 0$$

$$L_c = \frac{3\pi h^2}{4 H_0} \sqrt{\ln\left(\frac{A}{A_0}\right)} [-\varepsilon_0(1 + \nu)]^{-3/2}, \tag{27}$$

$$\frac{h}{H} \rightarrow \infty$$

Fig. 9 displays eq. (25), plotting L_c/H_0 as a function of h/H_0 at several values of ε_0 . We have set $\ln(A/A_0) = 5$ and $\nu = 0.3$ in plotting Fig. 9. For a given set of experimental conditions, the experimentally observed $L_c \approx 30\mu\text{m}$ [3], and the value read from Fig. 9 is $L_c = 20\mu\text{m}$. This agreement is gratifying, given how vague we are in declaring an island is critical in both the model and the experimental observation. In practice, Fig. 9 is perhaps more useful as an indication for trends. To fabricate large islands (L_c large), one should decrease ε_0 and increase h , if H_0 is held constant. For a given ε_0 , a proportional increase in H_0 and h will proportionally increase L_c , but keep relaxation time unchanged when $L = L_c$. Of course, the island

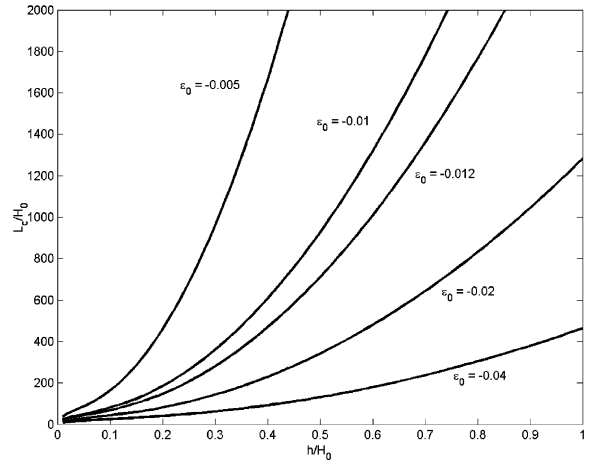


Fig. 9. The critical island size as a function of experimental variables.

thickness h is limited below a critical value to avoid threading dislocations. In the limit $h/H_0 \rightarrow 0$, when H_0 increases, t_E shortens but t_w remains unchanged, so that L_c increases. We caution that the conclusion is based on the shear lag model, which breaks down when the glass layer is too thick.

5. Stresses in the island and the viscous layer

5.1. Wrinkle-induced tension in the island

Cracks have been observed in the wrinkled islands [3]. The inplane stress at the top convex surface of the wrinkles has two contributions, one from the membrane strain and another from the bending curvature. The sum is

$$\sigma(x,t) = \frac{E\varepsilon_0}{1-\nu} + \frac{E}{1-\nu^2} \left[\frac{\partial u}{\partial x} + \frac{1}{2} \left(\frac{\partial w}{\partial x} \right)^2 \right] \tag{28}$$

$$- \frac{E}{1-\nu^2} \frac{\partial^2 w}{\partial x^2} \frac{h}{2}$$

We will evaluate the stress at the island center, denoted as σ^* . For short times, the stress is given by the linear perturbation analysis:

$$\sigma^* = \frac{E\varepsilon_0}{1-\nu} \frac{Ekh B(t)}{1-\nu^2 h} + \frac{E(kh)^2 A(t)}{2(1-\nu^2) h} \quad (29)$$

where $A(t)$ and $B(t)$ are the amplitudes of w and u , respectively. At the constrained equilibrium state, the stress is

$$\sigma^* = \frac{E(kh)^2}{2(1-\nu^2)} \left[\sqrt{\frac{1}{3} \left[\left(\frac{k_c}{k} \right)^2 - 1 \right]} - \frac{1}{6} \right] \quad (30)$$

The stress becomes tensile when the perturbation wavenumber is just slightly below the Euler critical buckling wavenumber, $k/k_c < \sqrt{12/13}$.

Fig. 10 shows σ^* as a function of time for islands of four sizes obtained from numerical simulations. As expected, the 15 μm island never has tensile stress in the entire process of relaxation. For the intermediate and large islands, the stress is initially compressive, but becomes tensile as the wrinkles amplify. This tensile stress builds up and reaches a maximum value. Cracks may nucleate anytime during the buildup of the tensile stress, depending on flaws in the islands. As the wrinkles begin to subside, the tensile stress decreases and turns slightly compressive before vanishing. Knowing the magnitude of the stress is insufficient to predict whether the island will crack. A fracture mechanics analysis similar to that for other thin film structures is needed [13]. We will pursue this in a later study.

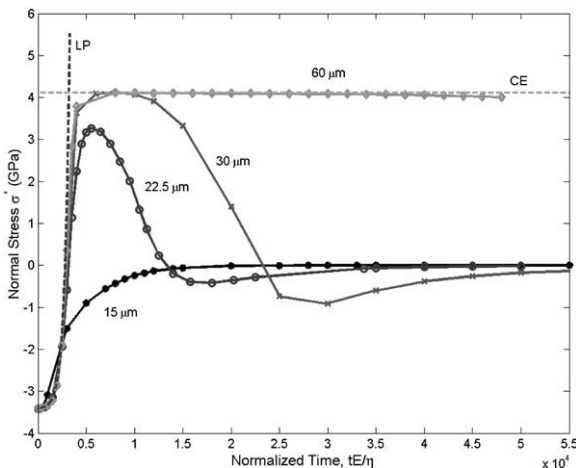


Fig. 10. Normal stress at the island center. LP: linear perturbation. CE: constrained equilibrium.

5.2. Hydrostatic stress in the glass layer

During annealing, the glass underneath the growing wrinkles will experience negative hydrostatic pressure, which may be significant enough to cause cavitation and debonding at the island-liquid interface, although this phenomenon has not been observed in experiments. Fig. 11 is a plot of the hydrostatic pressure at the island center. As the wrinkles increase in amplitude, a negative hydrostatic pressure of about 35 MPa builds up in the largest islands. For large islands, the pressure reduces as the islands approach the constrained equilibrium state.

6. Concluding remarks

This paper models the co-evolution of inplane expansion and wrinkling. Inplane expansion prevails in small islands. Relaxation quickly propagates from the island edges to the island center, and suppresses wrinkling. As for the larger islands, inplane expansion will still occur at island edges and eventually reach the center; however, by the time the inplane expansion arrives, the middle part of the island has already wrinkled substantially. The larger the island, the more time the wrinkles can amplify. Thus, a critical island size exists

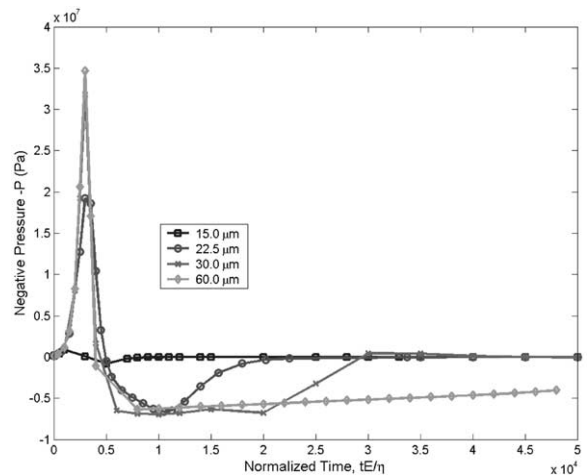


Fig. 11. The negative pressure in the glass layer caused by wrinkling.

below which inplane expansion prevails over wrinkling. This critical size depends on the misfit strain, the island thickness, and the glass layer thickness; however, it does not depend on glass viscosity. When the island wrinkles, we also show the tensile stress buildup in the island and the negative pressure in the glass. They may be used to assess the likelihood for wrinkle-induced fracture, debonding, and cavitation.

Acknowledgements

This work has been supported by the National Science Foundation, by the Department of Energy, and by the New Jersey Commission of Science & Technology.

References

- [1] Vanhollenbeke K, Moerman I, Van Daele P, Demeester P. Progress in Crystal Growth and Characterization of Materials 2000;41:1–55.
- [2] Hobart KD, Kub FJ, Fatemi M, Twigg ME, Thompson PE, Kuan TS, Inoki CK. Journal of Electronic Materials 2000;29:897–900.
- [3] Yin H, Sturm JC, Suo Z, Huang R, Hobart KD. Modeling of in-plane expansion and buckling of SiGe islands on BPSG. Presented at the 43rd Electronic Materials Conference, Notre Dame, Indiana, June 2001 (unpublished).
- [4] Freund LB, Nix WD. Appl. Phys. Lett. 1996;69:173.
- [5] Freund LB, Nix WD. (unpublished).
- [6] Sridhar N, Srolovitz DJ, Suo Z. Appl. Phys. Lett 2001;78:2482.
- [7] Huang R, Suo Z. Journal of Applied Physics, to appear in the 1 Feb., 2002 issue (Preprint available online at www.princeton.edu/~suo, Publication 120).
- [8] Huang R, Suo Z. Submitted to International Journal of Solids and Structures, 2001 (Preprint available online at www.princeton.edu/~suo, Publication 121).
- [9] Sridhar N, Srolovitz DJ, Cox BN. Submitted to Acta Materialia, 2001.
- [10] Reynolds O. Phil. Trans. Roy. Soc. London 1886;177:157.
- [11] Landau LD, Lifshitz EM. Theory of elasticity. London: Pergamon Press, 1959.
- [12] Timoshenko S, Woinowsky-Kreiger S. Theory of plates and shells, 2nd ed. New York: McGraw-Hill Inc, 1987.
- [13] Hutchinson JW, Suo Z. Advances in Applied Mechanics 1992;29:63–191.